CEAI, Vol. 5, No. 1, pp. 19-26, 2003 Printed in Romania

SLIDING MODE NAVIGATION CONTROL IN INTELLIGENT SPACE

Csongor SZABÓ(1), Péter KORONDI(2), Florin DRĂGAN(1) and Hideki HASHIMOTO(3)

(1)Politehnica University of Timi soara,1900, Timi soara, bd.Vasile Pârvan nr.2,Romania

e-mail:b624@aut.utt.ro

(2)Budapest University of Technology and Economics, H-1521, Budapest, P.O.Box 91, Hungary

e-mail:korondi@elektro.get.bme.hu

(3)Institute of Industrial Science, The University of Tokyo, 4-6-1 Komaba Meguro-ku Tokyo, Japan,e-mail:Hashimoto@hlab.iis.u-tokyo.ac.jp

Abstract *- This paper presents a general description for obstacle avoidance algorithms which can also describe the obstacle avoidance style(walking habit) of moving objects (human beings).A complex sliding mode based obstacle avoidance is presented as a test method, which is learned and modeled by the above mentioned general description. The paper presents simulation results of the sliding mode based navigation control.*

Keywords: *intelligent space, obstacle avoidance, potential field method vector field method, neuro fuzzy systems, sliding mode*

1. INTRODUCTION

The concept about robots has dramatically changed since mankind was able to accomplish certain basic aims in robot industry. From the image of intelligent machines which fascinated us in the science fiction literature to the real, autonomous working robot the path is long and complicated. That's why the early expectations from this field of science were high. Although there have been great progresses, robots which are capable of performing various and complex tasks in an autonomous and intelligent way, have not yet been able to conquer widespread applications. The design of the robots is influenced by the attempt to replicate human behaviors. The human behaviors are characterized by high complexity, for instance the human navigation is a very complex combination of very sophisticated sensing devices, and a more sophisticated sense of direction. For the robots there are two major possibilities. The first one is to use such highly developed vision and image sensing devices as the real "human" ones, but this method requires a huge computational power. The second way is to use less and simple sensing devices on the robot but to complete the hardware needs with such intelligent software that the robot can execute the required tasks in the expected way. In this paper, a sliding mode based motion control (obstacle avoidance behavior) is presented for a mobile robot in the Intelligent Space [1]. This motion control is learned by the

Intelligent Space by tracing the robot's movement [4] and thus learning its obstacle avoidance strategy. An adaptive, behavior learning is presented as a general method, a mathematical toolkit for learning different obstacle avoidance strategies. This learning is based on a neuro-fuzzy approximation for vector field based obstacle avoidance. The main aim of this paper is the presentation of the adaptive, behavior learning method and the sliding mode based obstacle avoidance method and the demonstration of the efficiency of the adaptive strategy, in the case of learning different complex methods among which there is the sliding mode based motion control too. This kind of efficiency in navigation is essential as among the main application tasks of the mobile robot like the example with the guidance of visually challenged people, which requests immediate response to any kind of disturbances. In the following section the concept of the Intelligent Space will be introduced and a short introduction to the basic theory for guiding styles will be drawn. In the third section a short description of the scalar based and the vector field based method for obstacle avoidance theory will be presented. The fourth section describes the sliding mode based obstacle avoidance behavior design. The last chapter shows the different experimental results of the presented algorithms.

2. INTELLIGENT SPACE AND BASIC OBSTACLE AVOIDANCE

Methods (Walking habits) Intelligent Space is a space (room, corridor or street), which has distributed sensory intelligence (various sensors, such as cameras and microphones with intelligence, haptic devices to manipulate in the space) and it is equipped with actuators [1]. Actuators are mainly used to provide information and physical support to the inhabitants. This is done by speakers, screens, pointing devices, switches or robots and slave devices inside the space. The various devices of sensory intelligence cooperate with each other autonomously, and the whole space has high intelligence [2], [4]. Each intelligent agent in the Intelligent Space has sensory intelligence [3]. The intelligent agent has to operate even if the outside environment changes, so it needs to switch its roles autonomously. The agent knows its role and can support man. Intelligent Space recomposes the whole space from each agent's sensory information, and returns intuitive and intelligible reactions to man. In this way, Intelligent Space is the space where man and agents can act mutually. There is an intelligent space, which can sense and track the path of moving objects (human beings) in a limited area. There are some mobile robots controlled by the intelligent space, which can guide blind persons in this limited area. The Intelligent Space tries to identify the behavior of moving objects (human beings) and tries to predict their movement in the near future. Using this knowledge, the intelligent space can help avoiding the fixed objects and moving ones (human beings) in the Intelligent Space. The proposed assistant mobile robot is shown on Fig.1.

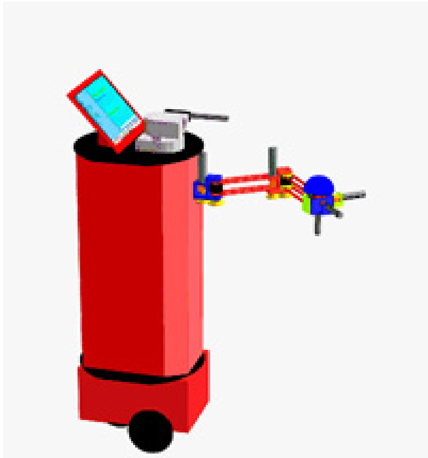

Fig. 1. - Guiding and Communication Assistant.

The base of the assistant robot is a mobile robot platform. This platform has a tricycle kinematics and drives along arcs, determined by steer angle α and speed v of the steered front wheel as shown on Fig.2.

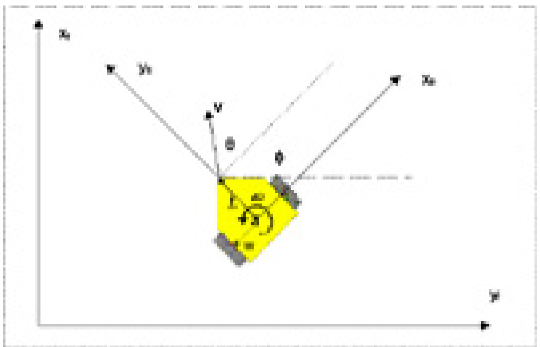

Fig. 2. - The tricycle kinematics of the mobile platform.

The robot needs plenty information about its surroundings. This information mostly provided by the Intelligent Environment. For the maximum safety the robot has own sensors mounted on the mobile platform. When the connection is lost with the Intelligent Environment, or the provided information is not reliable, then the robot uses its own sensor system. In the followings basic avoidance behaviors a re presented. Let us consider two extreme styles:

- The main guiding rule of an aircraft carrying dangerous material is to keep ”as far from the mountains as possible” •
- Remaining in secret while seeking a mouse leads to the opposite behavior for a cat, namely, ”get as close to the object as possible” Fig.3

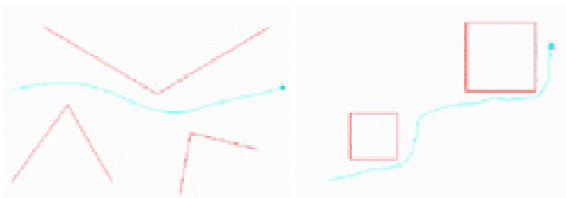

Fig. 3. - Basic Guiding Styles: “as far as possible” (left) “as close as possible” (right).

A simple combination of these can characterize the main rule of a traffic system: “keep close to right or left side”. A simple example to illustrate the importance of this knowledge. Let’s assume that a Japanese and an American person are walking towards each other. Recognizing this situation, they try to avoid each other. Using their general rule, the Japanese person keeps left and the American keeps right and they are again in front of each other. It might be ended in a collision (See Fig.4). If the Intelligent Space can learn the behavior of a human being, it can send a proper command to the robot in such situation.

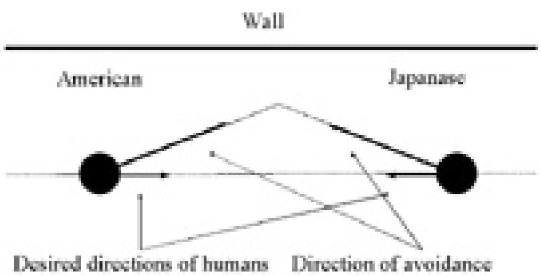

Fig. 4. - Example for problem of two different default avoidance.

3. SCALAR FIELD AND VECTOR FIELD BASED GUIDING MODEL

3.1. *Scalar field based method*

There are many approaches controlling mobile robots, interacting with a dynamic, uncertain environment [6], [7], [14], [8], and [9]. One of the widely adopted guiding style models is the potential based guiding (PBG) [6], [7], and [8]. The robot can detect objects in the scanned area (Fig.5).

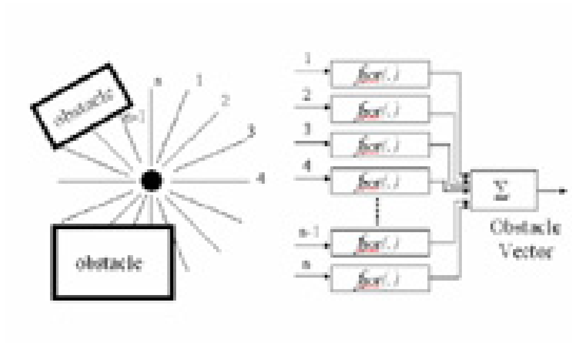

Fig. 5. - Sensor Area of the Robot (left), and the block diagram of the PBG (right).

The scanned area is divided into Z scanned lines that are pointed into directions of $-\vec{e}_z$ (unique vectors, where z = 1 . . .Z). The radial scanned lines structure has an important advantage that they density is growing with the decreasing distance to the robot. The sensor system provides the distance between the robot and the object on the scanned lines [12]. The main idea of the potential based guiding is to repulse (or attract) the robot from/to the obstacles, the artificial potential field having its global minimum for the goal and local maxima for the obstacles. The objects and the target generate imaginary forces acting on the robot. Summing the effect of these virtual forces, the desired moving direction can be obtained. The virtual vectors must be calculated for each location as quickly as possible to achieve a smooth and reactive guiding. The magnitudes of the repulsive forces are usually inversely proportional to the distance between the obstacles and the vehicle but they can be described by any non-linear functions. In many applications the same formula is used to compute all the repulsive forces, resulting a symmetrical potential field. In order to achieve different guiding styles asymmetrical potential fields may be used as well. A simple example for guiding style is the basic rule of traffic. The robots should keep to the right; therefore they must keep close to the obstacles on the right side while staying far from the objects on the left side. In most cases obstacles cause repulsive forces, but there are some examples where attractive object forces are desired. For instance when the robot must run close to a wall (which is a usual situation when the robots are used in corridors), this obstacle must attract the robot when the robot is too far from it. Potential functions that have negative sections, can achieve these kinds of styles. The main guiding rule of PBG is to repulse the robot from the objects [9], [10]. The process is divided into two blocks (see Fig.5). One defines the possible moving directions the second evaluates them. This means that the first block defines a moving vector

$$\vec{y}_z = \vec{e}_z \, w_z(x_z) \tag{1}$$

where Z = 1 . . .O (Z is the number of scanned lines, and O is the number of evaluated directions) from the measured distances x_z to each scanned lines. These vectors are pointed into the opposite of the scanned direction (key idea of PBG), and their absolute values depending on the detected distances are: $|\vec{y}_z| = w_z(x_z)$. This means that the potential function of the robot is sliced in the scanned directions (see Fig.5). Usually the evaluation is based on the sum operator that results in [8]:

$$\vec{y} = \sum_{z=1}^{Z=O} \vec{e}_z \, w_z(x_z), \tag{2}$$

In many cases this kind of evaluation is not effective. For example let the potential function on each scanned line be the same. Applying (2) to symmetrically located obstacles, will result in a zero vector. Choosing one of the $\vec{y}_z$ in the evaluation would lead to a better solution. In spite of the advantages the applicability of potential based guiding model is restricted by the fact, which has been noticed that its result strongly alternates incapable of guiding smoothly [7]. The key idea of potential based model is that the scanned object points repulse or attract the robot on the scanned line depending on the potential function. For instance, if the robot has to run parallel with a long wall the required vectors or at least their sum must be parallel with the wall. The PBG model is not able to generate such vectors (Fig.6).

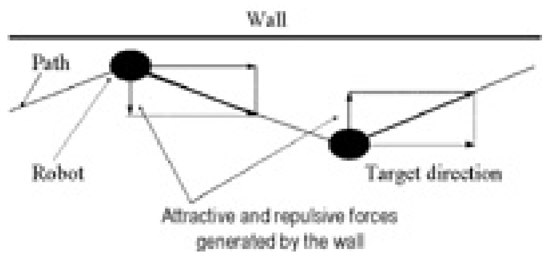

Fig. 6. - Guiding fluctuation of the PBG model

3.2. *Vector Field Based guiding model (VFB)*

This section extends the potential based guiding model to a vector field model, which defines a direction at every point of the potential surface (Fig.7).The proposed model is able to define arbitrary directions at each value of the measured distance on a scanned line. Therefore this model is able to generate output vectors that are parallel with a long wall located next to the robot.

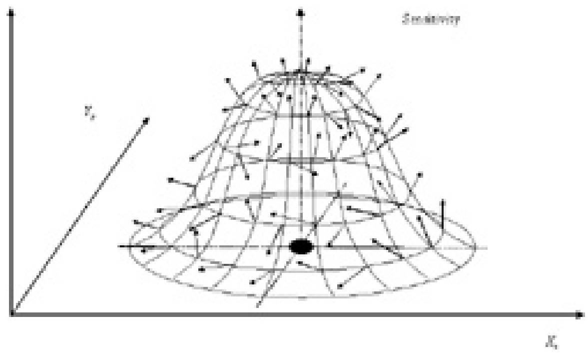

Fig. 7. - The VFB model.

The key difference from PBG is that all inputs of the first block have contribution to all outputs connected to the evaluation unit. Therefore, the potential field based model is a special case of 6

$$\vec{y}_z = \sum_{i=1}^{I=Z} w_{z,i} \, \vec{e}_i, \tag{3}$$

The moving vector, $\vec{y}$ can be expressed as the sum of the unit moving vector $\vec{y}_z$:

$$\vec{y} = \sum_{j=1}^{J+Z} \sum_{i=1}^{I=Z} w_{z,i} \, \vec{e}_i. \tag{4}$$

3.3. *General neural network modeling the VFB*

VFB model can be approximated by a generalized forward neural network that is general in the sense that it has various weighting functions set on the connections among the neurons [12]. In order to approximate the proper non-linear weighting functions $w_{z,i}(x_i)$ in the weighting units let us apply the proposed specialized fuzzy approach obtaining a neuro-fuzzy algorithm. Algorithm: Neuro-fuzzy based on the specialized fuzzy algorithm. Let weighting functions $w_{z,i}(x_i)$ be approximated by fuzzy sets as:

$$w_{z,i}(x_i) = \sum_{j=1}^{J} \mu_{A_{i,j}}(x_i) b_{z,i,j}. \tag{5}$$

From (3 and 5):

$$\vec{y}_z = \sum_{i=1}^{I} \sum_{j=1}^{J} \mu_{A_{i,j}}(x_i) = b_{z,i,j} \, \vec{e}_i . \tag{6}$$

4. SLIDING MODE BASED METHOD

This algorithm is based also on the drawing of a virtual potential field. Using the artificial potential field it is guaranteed a collision free trajectory along the gradient lines [15].From Fig.2. the motion equations of the robot can be deducted with respect to the fixed world frame (x_f, y_f) as follows:

$$\begin{aligned} \dot{x} &= v_G \cos\phi \\ \dot{y} &= v_G \sin\phi \quad , \\ \dot{\phi} &= v_G / L \tan\phi \end{aligned} \tag{7}$$

where v_G denotes the velocity vector at the center point of the mobile platform, constrained along the longitudinal axis attached to the robot due to the nonholonomic kinematics. A local harmonic potential field $\Psi(x, y)$ is constructed in the coordinate system attached to the robot (x_R, y_R) [16]. According to the Laplace equation this harmonic field satisfies:

$$\nabla^T \cdot \nabla\Psi(x,y) = \frac{\partial^2\Psi(x,y)}{\partial x^2} + \frac{\partial^2\Psi(x,y)}{\partial y^2} = 0 \tag{8}$$

The solution of (8) in a 2D Cartesian system (x, y) gives the potential of a singular point of strength q at (0,0):

$$\Psi(x, y) = q \ln \frac{1}{\sqrt{x^2 + y^2}} \tag{9}$$

and the associated gradient $\rho(x, y) \in \Re^2$:

$$\rho(x, y) = -grad\Psi(x, y) = \frac{q}{\sqrt{x^2 + y^2}} \begin{pmatrix} x \\ y \end{pmatrix} \tag{10}$$

A fundamental potential field configuration consist of a negative unit singular point in the goal and a positive singular point of strength $0 < q < 1$ in the obstacle center. $q = \dfrac{R}{R+e}$ from the equivalent point placement method, where e is the distance between the goal point and the obstacle center, and R is the radius of the circular obstacle security zone. As circular shaped obstacle security zones are inflexible to be employed directly [16] we will use elliptical security zones. We construct a harmonic potential field for each of the security ellipses with respect to the goal point. There is one security ellipse for each obstacle but in the case of more obstacles we use two ellipses one on each side of the selected path. In this case the two potential fields have to be fused somehow to form a single potential field. A good alternative method is to consider always only the closest security ellipse. Nevertheless this requires the switching of the potential fields when crossing the equidistant lines between the ellipses. This switching causes a discontinuous gradient field as illustrated in Fig.8.

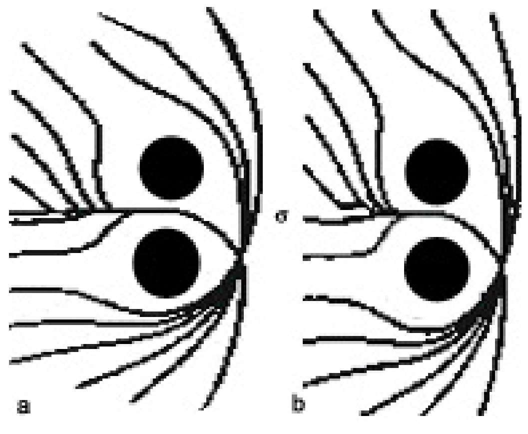

Fig. 8. Gradient lines for discontinuous gradient switching:

a) discontinuous switching; b) smooth switching.

In this case the sliding surface can be described by the equidistant line $\sigma_{eq} = 0$.Chattering appears as oscillations when switching between gradient lines. This effect can be reduced by smoothing the gradient lines in the vicinity of the equi-distance line by space domain smoothing [16] in the boundary layer along the equi-distance line between the two security zones, the resulting smooth gradient field's gradient being the weighted sum of the two gradients for each obstacle configuration. For the mobile platform on Fig.2. the control inputs are v and α but in general these two are the output of some actuator [16].Unmodeled dynamics is considered to be the major cause for chattering in real-life applications but in this case we assume that the actuators are ideal without dynamics. As used already above, the gradient $\rho(x, y)$ is implemented as a velocity field. The kinematics constrains the robots motion from three dimensional to two dimensional along velocity vector. It's assumed that the state variables x, y, ϕ and the kinematical parameters L and W are known. The scope to follow is to control the orientation of the angle ϕ of the cart to be co-linear to the gradient $\rho(x, y)$. So the desired orientation at (x, y) is:

$$\phi_\rho = A\tan\frac{\rho_y}{\rho_x} \quad with \quad \rho(x,y) = \begin{pmatrix} \rho_x \\ \rho_y \end{pmatrix} \in \Re^2 . \quad (11)$$

As the velocity control is straightforward the desired direction of motion is determined by β, $v = \beta|\vec{v}|$, where β is defined with the orientation error $\Delta\phi$, as follows:

$$\begin{aligned}
&\Delta\phi = \phi_\rho - \phi + 2\pi \Rightarrow \beta = 1\, if\ -2\pi < \phi_\rho - \phi < -\frac{3\pi}{2} \\
&\Delta\phi = \phi_\rho - \phi + \pi \Rightarrow \beta = -1\, if\ -\frac{3\pi}{2} < \phi_\rho - \phi < -\frac{\pi}{2} \\
&\Delta\phi = \phi_\rho - \phi \Rightarrow \beta = 1\, if\ -\frac{\pi}{2} < \phi_\rho - \phi < \frac{\pi}{2} \\
&\Delta\phi = \phi_\rho - \phi - \pi \Rightarrow \beta = -1\, if\ \frac{\pi}{2} < \phi_\rho - \phi < \frac{3\pi}{2} \\
&\Delta\phi = \phi_\rho - \phi - 2\pi \Rightarrow \beta = 1\, if\ \frac{3\pi}{2} < \phi_\rho - \phi < 2\pi
\end{aligned} \quad (12)$$

The sliding surface for the orientation error is defined as:

$$\sigma = \beta\Delta\phi . \quad (13)$$

Sliding mode is established along the surface $\sigma = 0$ but at the same time switching of the direction of the motion, switching the sign of β has to be avoided. This can be avoided by monotonously decreasing $\Delta\phi$ by controlling the value of ϕ [16].

The positive definite quadratic form $V = \frac{1}{2}\sigma^T\sigma$ [16] is used as the Lyapunov function candidate in this case. Differentiating this function along the system trajectories:

$$\sigma^T\dot{\sigma} = \sigma^T v\left(S\cos\theta - \frac{1}{L}\right). \quad (14)$$

where,

$$S(x,y,\phi) = \frac{\rho_x\frac{\partial p_y}{\partial x} - \rho_y\frac{\partial p_x}{\partial x}}{\|\rho^2\|}\cos\phi + \frac{\rho_x\frac{\partial p_y}{\partial x} - \rho_y\frac{\partial p_x}{\partial x}}{\|\rho^2\|}\sin\phi . \quad (15)$$

describes the rate of change of curvature of the gradient along the trajectory lines. If we define $\varphi = \arctan SL$ then (14) becomes:

$$\sigma^T\dot{\sigma} = \sigma^T v\sqrt{S^2 + \frac{1}{L^2}}\sin(\varphi - \theta) \quad (16)$$

where,

$$\sin(\varphi - \theta) = -\beta\, sign\sigma = -sign\Delta\phi . \quad (17)$$

Solving this equation for θ:

$$\theta = \varphi + \frac{\pi}{2} sign\Delta\phi . \quad (18)$$

From 16 and 17:

$$\sigma^T\dot{\sigma} = -|v|\sqrt{S^2 + \frac{1}{L^2}}\,|\sigma| \quad (19)$$

The convergence of σ to 0 can be achieved by examining the in-equation:

$$\frac{d}{dt} \le -4G(t)V^{\frac{1}{2}} \quad (20)$$

with,

$$G(t) = |v(t)|\sqrt{S^2 + \frac{1}{L^2}} \quad (21$$

for $v > v_{\min} \Rightarrow G(t) > G_{\min} = \frac{v_{\min}}{L}$,the time solution of (20) is given by:

$$V(0)^{\frac{1}{2}} - V(t)^{\frac{1}{2}} = 2\int_0^t G(\tau)d\tau \quad (22)$$

For $t \geq t_{\min} = \dfrac{V(0)^{\frac{1}{2}}}{2G_{\min}} \Rightarrow |\Delta\phi| = 0$ and an exact tracking of the gradient is guaranteed. Motion equations will be reduced to:

$$\begin{aligned} \dot{x} &= v\frac{\rho_x}{\|\rho\|}\cos\theta = v\frac{\rho_x}{\|\rho\|}\sin\varphi sign\Delta\phi \\ \dot{y} &= v\frac{\rho_y}{\|\rho\|}\sin\theta = v\frac{\rho_y}{\|\rho\|}\cos\varphi \end{aligned} \tag{23}$$

5. EXPERIMENTAL RESULTS

If we propose a trajectory which we gained with the sliding mode control method shown on fig. a, the experimental results obtained from simulations of the PBG and the VFB based models are shown on the fig. b. and the fig. c. The results show that the VFB based learning model gives a more precise learning of the presented strategy sample than the PBG model. The next step of the research will be the comparison of the sliding mode control based obstacle avoidance strategy and the learned VFB based strategy in different situations in the intelligent space.

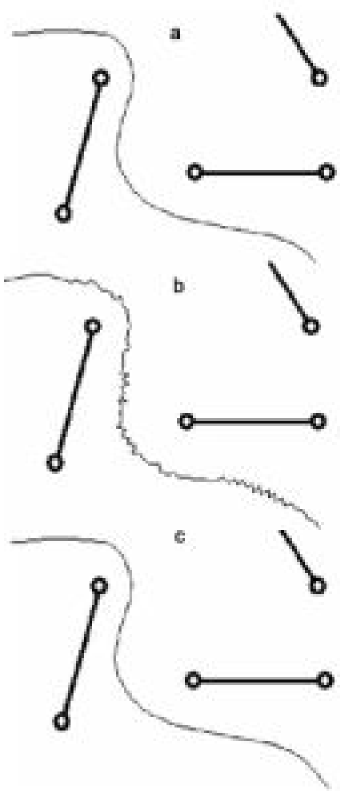

Fig. 9. - Experimental results: a) Sliding mode based model; b) PBG based model; c) VFB based model.

6. CONCLUSIONS

As we can see from the presentation of the different methods, the sliding mode based obstacle avoidance algorithm is a complex avoidance strategy much more complicated than the simple behavior based models. Although this complexity the PBG based model gives a good approximation of this behavior in simple cases. It is shown also that the VFB based model gives even a better solution in this case. In the followings of the research we will test the efficiency of these models in more complicated situations with numerous obstacles.

7. REFERENCES

[1] Lee, J.-H. and Hashimoto, H. - "Intelligent Space - Its concept and contents", *Advanced Robotics Journal*, Vol. 16, No. 4, 2002.

[2] Akiyama, T., Lee, J.-H. and Hashimoto, H. - "Evaluation of CCD Camera Arrangement for Positioning System in Intelligent Space", *International Symposium on Artificial Life and Robotics*, 2001.

[3] Morioka, K., Lee, J.-H. and Hashimoto, H. - "Human Centered Robotics in Intelligent Space", *2002 IEEE International Conference on Robotics and Automation (ICRA'02)*, pp. **2010-2015**, May, 2002.

[4] Morioka, K., Lee, J.-H. and Hashimoto, H. - "Physical Agent for Human Following in Intelligent Sensor Network", *2002 IEEE/RSJ International Conference on Intelligent Robotics and Systems (IROS'02)*, pp. **1234-1239**, Oct., 2002.

[5] Dozier, Homaifar, Bryson and Moore - "Artificial Potential Field Based Robot Navigation Dynamic Constrianed Optimization, and Simple Genetic Hill-Climbing", In the *ICEC '98 Proceedings*, 1998.

[6] Koren, Y. and Borenstein, J. - "Potential Field Methods and Their Inherent Limitations for Mobile Robot Navigation", *Proc. of the IEEE Int. Conf. on Robotics and Automation*, pp. **1398-1404**, 1991.

[7] Kubota, N., Morioka, T., Kojima, F. and Fukuda T. - "Sensory Network for Fuzzy Controller of a Mobile Robot", *Proc. FUZZ-IEEE 1999*, Vol 2, pp. **986-991,** 1991.

[8] Bronstein, J. and Koren, Y. - "Real-time obstacle avoidance for fast mobile robots", *IEEE Transactions on Systems Man and Cybernetics*, vol.19, no. 5, pp. **1179-1187**.

[9] Arkin, R.C. - "Motor Schema-Based Mobile Robot Navigation", *International Journal of Robotics Research*, Vol. 8, No. 4, August 1989, pp. **92-112**, 1989.

[10] Mizumoto, M. - "Fuzzy controls by Product-sum-gravity method", *Advance-ment of Fuzzy Theory and Systems in China and Japan*, Eds. Liu and Mizumoto, International Academic Publishers, c1.1-c1.4, 1990.

[11] Nagy, I., Fung, W.K. and Baranyi, P. - "Neuro-Fuzzy based Vector Field Model: An Unified Representation for Mobile Robot Guiding Styles", *IEEE Int. Conf. System Man and Cybernetics (IEEE SMC'2000)*, Nashville, Tennessee, USA, pp. **3538-3543**, 2000.

[12] Baranyi, P., Yam, Y., Varkonyi-Koczy, A., Patton, R.J., Michelberger, P. and Sugiyama, M. - "SVD Based Reduction to TS Fuzzy Models", *IEEE Transaction on Industrial Electronics*, Vol. 49, No. 2, pp. **433-443**, 2002.

[13] Luo, R.C., Chen, T.M. and Yin C.-C. - "Intelligent Autonomous Mobile Robot Control through the Internet", *ISIE 2000*, Cholula, Puebla, Mexico, 2000.

[14] Guldner, J. and Utkin, V.I. - "Sliding mode control for an obstacle avoidance strategy based on an electrical potential field", In *Proc. IEEE Conf. Decision and Control*, (San Antonio, TX, USA), pp. **424-429**, 1993.

[15] Guldner, J., Utkin V.I. and Bauer, R. – "Sliding mode navigation control for nonholonomic mobile robots", In *PROC. Asian Control Conference*, Tokyo, pp. **393-396**, 1994.